coatings

MDPI

Article

Temperature and Flexural Endurances of Aluminum-Doped Zinc Oxide Thin Films on Flexible Polyethylene Terephthalate Substrates: Pathways to Enhanced Flexibility and Conductivity

Mohammad M. Hamasha [1,*], Sa'd Hamasha [2], Khalid Alzoubi [3], Mohammed Said Obeidat [4] and Raghad Massadeh [5]

[1] Department of Industrial Engineering, Faculty of Engineering, The Hashemite University, Zarqa 13133, Jordan
[2] Department of Industrial Engineering, School of Applied Technical Sciences, German Jordanian University, Amman 11180, Jordan
[3] Department of Industrial Engineering, Faculty of Engineering, Jordan University of Science and Technology, Irbid 22110, Jordan
[4] College of Engineering and Technology, American University of the Middle East, Egaila 54200, Kuwait
[5] Department of Chemistry, Faculty of Science, Yarmouk University, Irbid 21163, Jordan
* Correspondence: mohamad_hamasha@yahoo.com; Tel.: +962-5-390-3333 (ext. 4679)

Abstract: This work investigates the endurance and performance of aluminum-doped zinc oxide (AZO) thin films fabricated on flexible polyethylene terephthalate (PET) substrates, providing new insights into their degradation linked to mechanical flexing and accelerated thermal cycling (ATC). The current study uniquely combines cyclic bending fatigue at 23 °C and 70 °C with ATC between 0 °C and 100 °C, simulating operational stresses in real-world environments, in contrast to previous research that has focused primarily on either isolated mechanical or thermal effects. The 425 nm thick films showed high transparency and conductivity, making them suitable materials for flexible electronics and optoelectronic devices. In this work, electrical resistivity, one of the most important performance parameters, was investigated after each mechanical or thermal cycle. The results indicate that mechanical cycling at high temperatures can drastically enhance the crack formation and electrical degradation, with an over 250% change in the electrical resistance (PCER) after 12,000 cycles at 70 °C and more than 300% after 500 thermal cycles. The highly deleterious effects of combined stressors on the structural integrity and electrical properties of AZO films are underlined by these observations. This study further suggests that the design of more robust AZO-based materials/coatings would contribute toward achieving better durability in flexible electronic applications. These findings also go hand in glove with the ninth goal of the United Nations' Sustainable Development Goals, specifically Target 9.5: Enhance Research and Upgrade Industrial Technologies.

Keywords: aluminum-doped zinc oxide; AZO; flexible electronics; cyclic bending fatigue; thermal cycling; electrical resistivity degradation

check for updates

Citation: Hamasha, M.M.; Hamasha, S.; Alzoubi, K.; Obeidat, M.S.; Massadeh, R. Temperature and Flexural Endurances of Aluminum-Doped Zinc Oxide Thin Films on Flexible Polyethylene Terephthalate Substrates: Pathways to Enhanced Flexibility and Conductivity. *Coatings* **2024**, *14*, 1527. https://doi.org/10.3390/coatings14121527

Received: 9 November 2024
Revised: 27 November 2024
Accepted: 30 November 2024
Published: 3 December 2024

Copyright: © 2024 by the authors. Licensee MDPI, Basel, Switzerland. This article is an open access article distributed under the terms and conditions of the Creative Commons Attribution (CC BY) license (https://creativecommons.org/licenses/by/4.0/).

1. Introduction

Transparent conductive oxide (TCO) films find indispensable applications in photovoltaics [1–3], liquid crystal displays (LCDs) [4,5], organic light-emitting diodes (OLEDs) [6], and sensors [7] owing to their highly conductive electrical and optically transparent properties, making them suitable for devices requiring light transmission with electrical functionality. For such applications, good performance requires both low electrical resistivity—essential for photovoltaic efficiency [8]—and an optical bandgap of greater than 3 eV, with transparency exceeding 85% [9]. These properties must be harmoniously combined in TCO films to achieve high-performance optoelectronic devices.

Recently, the development of flexible electronics has started to lead to wider uses of TCO films deposited on flexible substrates. These films find applications in wearable

devices, foldable displays, and other technologies of the future [10]. In practice, their integration is problematic because of mechanical stresses that are encountered in the process of manufacturing, operation, and environmental exposure. In order to ensure durability and long-term performance, the responsiveness of TCO films to mechanical stresses—including bending, stretching, and compression—is being studied, together with environmental conditions, such as fluctuations in temperature and humidity [11]. It is generally important to simulate reality under controlled experimental conditions in order to understand and improve TCO films' reliability in flexible systems [12]. Mechanical loading tests—e.g., cyclic bending and thermal cycling—help to evaluate their flexibility, toughness, and recovery from deformation [13].

Mechanical stresses impact TCO films by inducing microcracks, delamination, and degradation in electrical properties, thereby compromising device performance. Understanding these mechanical–electrical interactions is essential, as defects, like microcracks, can disrupt conductive pathways and reduce device reliability [14]. This work is of particular relevance for applications that demand performance consistency: wearable medical devices, flexible solar panels, and foldable displays to name a few. Indeed, investigations into TCO films' behaviors under dynamic mechanical and environmental conditions provide insights into critical improvements for material properties and drive innovation in flexible electronics. Cyclic bending and thermal cycling are among common methods used to investigate the durability of TCO films. Cyclic bending simulates repetitive mechanical deformations encountered in device use, and the researcher is allowed to monitor crack formation, resistance changes, and structural integrity under stress [15–18]. Thermal cycling involves exposing the films to alternating temperatures that simulate thermal strains occurring in real-world environments [19,20]. Such experiments have been performed to study TCO films' reliability by characterizing changes in electrical resistance, crack density, and structural deformation to assist in applying these films to flexible systems.

Among TCO materials, aluminum-doped zinc oxide (AZO) has emerged as a promising alternative to indium tin oxide (ITO). The use of scarce indium resources and the possible exhaustion of these resources within a few decades have motivated the research of sustainable alternatives. Made of zinc oxide doped with aluminum, AZO presents crystal structures and bandgaps similar to those of ITO at a lower cost and greater availability than ITO [21]. These advantages make AZO an attractive option for large-scale production in photovoltaics, displays, touch screens, and OLEDs. In addition, AZO films are characterized by high visible-light transparency, with low electrical resistance that can be applied in flexible electronics [22].

Extensive efforts have been made to study AZO's properties and deposition methods. Zhang et al. [23] analyzed a series of advanced devices using inductively coupled plasma analysis, X-ray spectroscopy, X-ray photoelectron spectroscopy, and UV–visible spectroscopy for samples of aluminum-doped zinc oxide powder prepared using an active surface material complex sol–gel method. X-ray diffraction showed that the nanoparticles were impurity-free at a processing temperature of 1273 K and possessed a purely hexagonal structure. The optical energy gap was found to lie between 3.2 eV and 3.5 eV, depending on the concentration of the aluminum added. Zhou et al. [24] used the sol–gel dip-coating method to deposit polycrystalline AZO films, finding that heat treatment at 500 °C enhanced crystallinity and reduced resistivity to 1.5×10^{-3} Ω·cm. By the same token, Radhouane Bel Hadj Tahar [25] indicated that a 2% aluminum doping level optimized both the crystallinity and electrical properties, achieving a resistivity of 5.4×10^{-3} Ω·cm. Various deposition techniques—like radio frequency (RF) magnetron sputtering [26], which achieves a resistivity as low as 2×10^{-3} Ω·cm with excellent layer uniformity; DC magnetron sputtering [27], which allows for deposition at temperatures as low as 200 °C; and molecular beam epitaxy (MBE) [28], pulsed-laser deposition (PLD) [29], and sol–gel processes [30], which facilitate low-temperature deposition with resistivity values around 3×10^{-3} Ω·cm—offer superior results based on application-specific needs. For example, RF magnetron sputtering is particularly useful for controlling layer thickness and unifor-

mity, while the sol–gel process is advantageous for low-cost, low-temperature deposition on flexible substrates. This flexibility in techniques has been a factor in establishing AZO as the front-runner material among TCO materials.

The objective of the present work is to study the mechanical and electrical properties of AZO films deposited on flexible substrates. AZO films (425 nm thick) were deposited on 127 μm thick polyethylene terephthalate substrates by RF magnetron sputtering. Cyclic bending was performed at room temperature and at elevated temperatures; the surface morphology, after bending, was studied in order to estimate the crack generation. Electrical resistivity was evaluated following bending cycles of 100, 200, and up to 1200. The experiments were designed using a DOE approach, and the results were evaluated through analysis of variance. Thermal cycling tests were conducted to investigate the thermal effects on the films and substrates. Detailed findings give valuable insights into the durability of AZO films and their potential for flexible electronic applications.

The novelty of this study is that it covers a field investigation into the combined effects of cyclic bending fatigue and thermal cycling on AZO thin films, simulating real-world operational stresses. This work, compared to most previous studies, which are focused on either the isolated mechanical or thermal factor, opens new avenues for understanding the degradation mechanism of AZO films at elevated temperatures and under repeated mechanical stresses, thus offering actionable solutions for enhancing durability in flexible electronics and optoelectronic applications.

2. Experimental Design

In this paper, an experimental design is presented to carry out a detailed study on the durability and performance of AZO thin films deposited on flexible substrates under mechanical and thermal stresses. Each one of the experimental procedures was designed in such a way that the effects of the cyclic bending fatigue and thermal cycling on the electrical and structural properties of these thin films are systematically explored for their use in flexible electronic applications.

The major parts of this research consisted of mechanical stress simulations by bending fatigue testing, which flexible electronics would undergo during operation, and accelerated thermal cycling (ATC) to study the behavioral variation at every temperature change. Such integration of experiments could help to establish a comprehensive understanding of the reliability and performance degradation mechanisms of AZO thin films upon exposure to real application conditions. The preparation of the samples, test protocols, and analysis of the data were carried out by adopting standardized methodologies, which, in turn, ascertain the validity and reproducibility of the results. The methodologies adopted for the fabrication of the AZO thin films and the experimental procedures followed for the cyclic bending fatigue and ATC tests are discussed in the following subsections.

2.1. AZO Thin Film Preparation

AZO thin films (425 nm thick) were exactly deposited on top of 127 μm thick polyethylene terephthalate (PET) substrates using RF magnetron sputtering. Reference [31] reported that the optical bandgap decreased from 3.95 eV to 3.80 eV as the thickness of the AZO film increased from 100 nm to 500 nm, indicating that the films remain highly transparent. PET substrates were chosen on purpose for their specific features and clean uncoated surface for facilitating the exact analytical AZO deposition without additional layers. The reliability of the quality of thin films requires a high-quality target of AZO with a 2″ diameter × 1.25″ thickness. The targets (98% ZnO and 2% Al_2O_3 by weight; 99.99% pure) were obtained from Plasmaterials, Inc. The substrate coatings of AZO were preserved through the high target purity, which had the most profound effect on the experimental results. The substrate preparation was just as important: Cleaning the substrates ultrasonically with acetone, ethanol, and distilled water removed impurities. These processes were timed to ensure purity, followed by drying the substrates with nitrogen gas prior to sputtering. The vacuum chamber was prepared, at a base pressure of 3×10^{-5} Torr,

for the RF magnetron sputtering optimization. Sputtering at room temperature was conducted under identical conditions. During operation, a power input of 75 W, an argon flow rate of 100 standard cubic centimeters per minute (SCCM), and a chamber pressure of 1×10^{-2} Torr were maintained. Pre-sputtering was allowed to run for 5 min to attain the desired atmosphere; then, the substrate holder was spun at 22 revolutions per minute to support the even deposition of the layers. One of the side effects of RF magnetron sputtering is target material contamination, which will introduce impurities to deposited films. It may also heat the substrate during processing, causing thermal stress or deformation of flexible substrates and impairing the adhesion of films and the overall structural integrity. Solar cell applications need resistivity and optical transmission; hence, 425 nm thick AZO thin films were chosen. The choice of the 425 nm thickness for the AZO layer is based on the optimal balance between optical transparency and electrical conductivity. AZO films are transparent within a broad thickness range, including 425 nm, which provides sufficient light transmission for applications, such as solar cells. On the other hand, the 425 nm thickness is sufficient to provide low electrical resistance, which, in turn, allows for good charge transport. The combination of these high transparency and low resistivity properties makes 425 nm the ideal thickness when high values are needed for both optical and electrical performances. The films and substrates used in this study were 8-inch-long, 0.5-inch-wide, 425 nm thick AZO-films, and 127 μm thick rectangular PET substrates. The film thickness was estimated using a quartz crystal microbalance (QCM), widely adopted as a device that is usually combined together with sputtering systems. QCMs depend on measuring the changes in the vibrating frequency of a quartz crystal. During the sputtering process, material is deposited onto the crystal by increasing its mass and lowering its vibrating frequency. This frequency shift is directly correlated with the thickness of the deposited film, allowing for precise in situ measurements.

2.2. Cyclic Bending Fatigue Experiment

The test vehicle has two layers of 425 nm thick AZO thin films atop a 127 μm thick PET substrate. A total of 88 samples were used in the experiment. Each sample received midway cyclic bending, as detailed below, at a rate of 67 cycles/minute. The sample dimensions were 8 inches long and 0.5 inches wide. Each sample was attached to a plastic strip to create a loop, with a 75 g mass placed on the opposite end of the strip. Furthermore, copper tape was applied to both ends of the sample to measure the electrical resistance. The maximum sample displacement between neutral and extreme positions was 2 cm. A controlled-chamber-based flexible electronic fatigue tester was employed for this study. Figure 1a shows how to hold one or two bending mandrels of various diameters. The two-mandrel design with a 2-inch diameter was used. The sample is repeatedly bent from both sides in this configuration. During rotor rotation, the bending mandrels reciprocate vertically, bending the sample around them. The sample bends upward around the lower mandrel during the upstroke (Figure 1b) and downward around the top mandrel during the downstroke (Figure 1c). The specimen bends around the mandrels as the weight softly stretches it.

This bending process causes tensile and compressive stresses on the thin film as the sample bends against the substrate and thin film sides. Repeated tension and compression cycles increase the number of sample cracks and electrical resistance. Half of the samples were tested at 23 °C to replicate room temperature and half at 70 °C to see how increased temperatures accelerate thin film crack formation.

Starting with the first 5 samples tested at 23 °C, and the 5 tested at 70 °C, the electrical resistance was measured after every 100 cycles, up to 1200 cycles. The 10 samples resulting from this step were used for plotting the curve for the relationship between the number of cycles and the resistance. The remaining 78 samples were reserved for the design of the experiment (DOE), as described in Section 2.4.

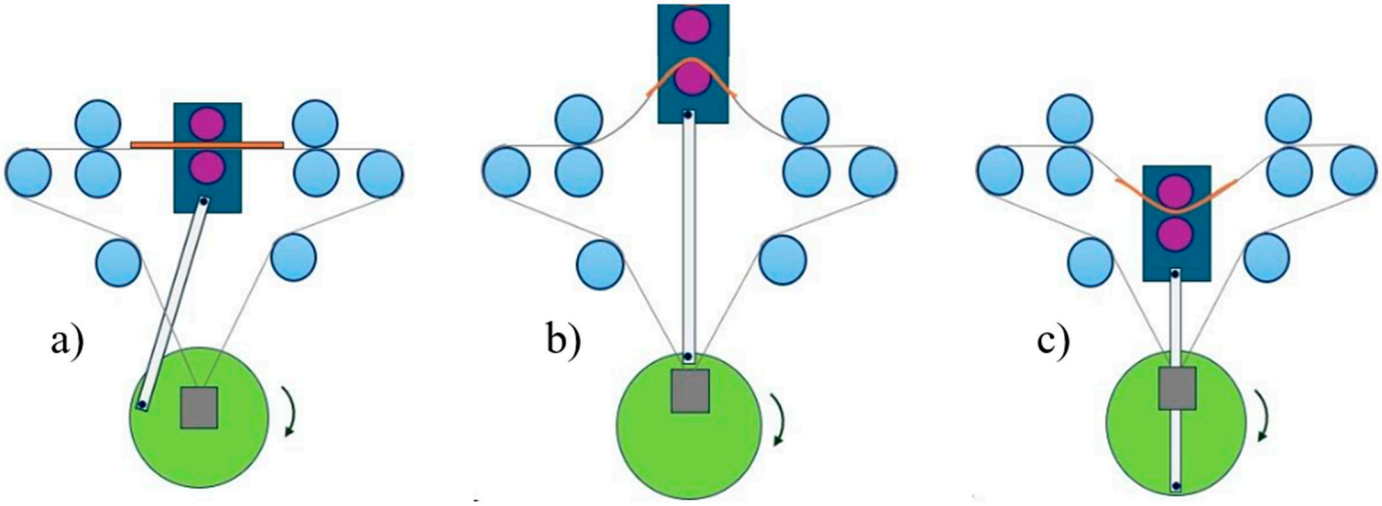


Figure 1. Bending fatigue tester setup showing the two-mandrel design used to apply cyclic tensile and compressive stresses to AZO thin films: (**a**) flat sample, (**b**) bent around lower mandrel, and (**c**) bent around the upper mandrel.

2.3. Electrical Resistance Measurements

The electrical resistance measurements were performed using a precision multimeter, model: Keithley 2450 Source Meter from (Tektronic UK Ltd, Bracknell, UK). Copper tape was attached to both ends of the samples for stable electrical contacts during the measurements. This setup was used to monitor the resistance changes in the course of the experiment. The resistance measurements were conducted after certain intervals of cyclic bending or thermal cycling, as mentioned in the DOE section.

The electrical degradation of the AZO thin films was quantified by calculating the percentage change in the electrical resistance (PCER), using the following expression in Equation (1) (Refs. [31,32]):

$$PCER = \frac{R - Ro}{Ro} \times 100\% \quad (1)$$

The value of the PCER is representative of the degradation of the electrical properties of the AZO thin films after cyclic bending and thermal cycling. In the equation, R is the electrical resistance after the applied bending cycles or thermal stress, while Ro is the initial resistance of the sample. This provided a consistent way to compare the different samples regarding the effects of the mechanical and thermal stresses. The resistance measurements were made in a controlled environment to minimize noise issues and to guarantee repeatability.

2.4. DOE

The influences of the main factors, such as the number of cycles and the temperature, were investigated by making use of the DOE tool. Whereas it is assumed that the number of cycles will affect the PCER, the extent to which it will do so and, more importantly, the effect of the temperature, along with that of the interaction between the temperature and the number of cycles, on the PCER are unknown; hence, the DOE will be imperative in explaining these matters.

To implement a sound DOE, each factor was given some specified levels. Cycles of deformation were in steps of 0, 100, 200, and up to 1200, and temperatures were 23 and 70 °C. Thus, this results in a total of 26 different treatment combinations. Each treatment was replicated three times to provide a total of 78 experimental runs. All the experiments were conducted in a randomized sequence to avoid unwanted variation. These were followed by analyses for variance, main effects, and interaction effects of the experiments, which results were then presented graphically. ANOVA on the results obtained following the DOE design was then performed. In conducting the ANOVA, data from all 78 experimental

runs were collected. To minimize any possible noise, the experimental runs were arranged in a random manner. Data collection was followed by a mixed full factorial design using MINITAB-17 software. From here, the results of the ANOVA were determined using the number of cycles and the temperature as factor variables, and their influences on the PCER were determined. Main effect plots, interaction effect plots, and surface plots were generated too.

2.5. ATC Experiment

The same 10 AZO/PET samples were utilized in the bending fatigue tests and ATC studies. The studies were conducted in a Thermatron environmental chamber, which can reach from −73 °C to 177 °C. The ASTM E1171-01 solar module cyclic temperature and humidity test technique was followed. The samples were mounted on stands and placed in a nitrogen-filled room to avoid moisture. Following the profile in Figure 2, the samples were thermally cycled between 0 °C and 100 °C at 10 °C per minute, with a 10-minute pause at the extremes. The ATC experiment was ended after 500 heat cycles. The sheet resistance from the end of the sample was measured at the start and after 50, 100, 150, 300, 350, and 500 cycles for all the samples. After each measurement point, the chamber was stopped, and the samples were removed and cooled before measuring the resistance and then returned to complete the test.

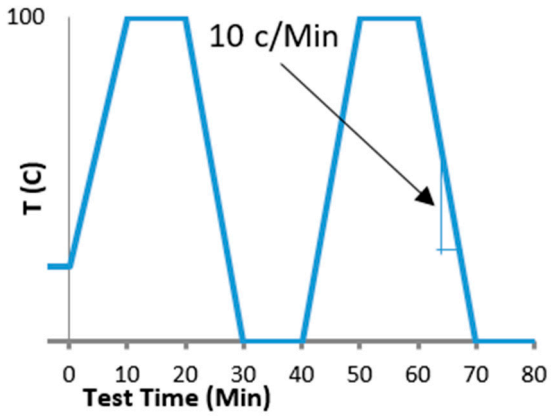


Figure 2. Thermal cycling profile used in the ATC tests, showing temperature shifts between 0 °C and 100 °C, with a 10-minute dwell time.

2.6. SEM and Optical Microscopy

The structural and surface morphologies of the AZO thin films were studied using scanning electron microscopy (SEM) and optical microscopy. The SEM analyses were carried out in a Sigma 360 VP SEM, ZEISS, (Oberkochen, Baden-Württemberg, Germany) with secondary electron and backscatter electron detectors to capture detailed microstructural features. Cross-sectional samples were embedded in resin, sectioned by means of an ultra-microtome, and mounted on conductive stubs to ensure high-resolution imaging. SEM provided critical insights into the columnar growth structure in the films and the development of cracks subsequent to mechanical or thermal stress.

The surface morphology, both before and after cyclic bending or thermal cycling, was further investigated using an optical microscope (ZEISS Axiovert 5 digital). Surface imperfections, microcracks, and reflectivity changes indicative of refractive index and microstructural uniformity changes were observed using the optical microscope. Images were taken in the magnification range from 100× to 500× to document surface changes during the experiments.

SEM and optical microscopy were used in combination and proved to be indispensable for characterizing the structural integrity and understanding the degradation mechanisms of the AZO films under superimposed mechanical and thermal stresses.

3. Results and Discussion

Figure 3 shows the microstructure of the as-made AZO thin film. The SEM image shows the columnar growth of the AZO thin layer on the left side. The thin film is deposited in layers, with a homogeneous and well-aligned columnar architecture, as shown by the 425 nm thick vertical structures. Sputtered films grow column-like under the correct deposition conditions.

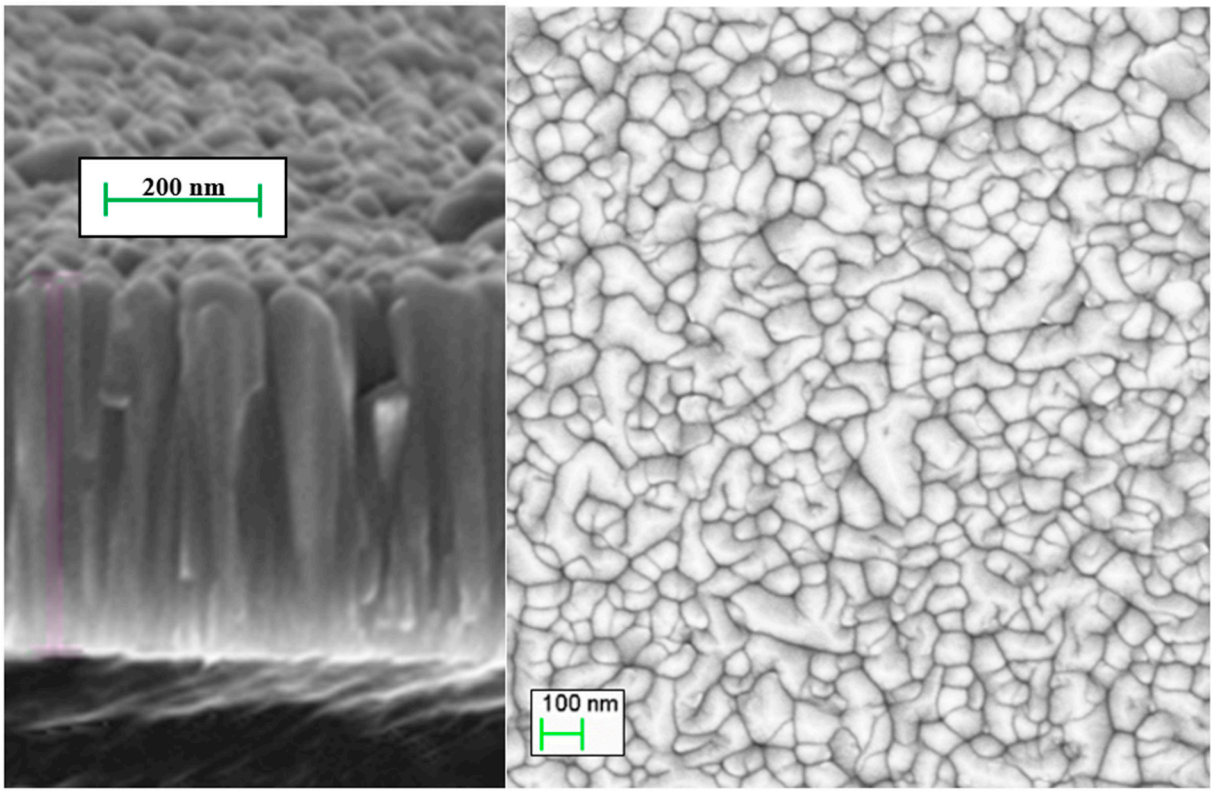


Figure 3. SEM images of the 425 nm thick AZO film: cross-section (**left**) showing columnar structure and top view (**right**) displaying closely packed grains.

In detail, Figure 3 (right) presents the top view SEM image, showing closely packed grains with irregular shapes. These grains are responsible for the high electrical conductivity and transparency of the film. The columnar structure observed in the cross-sectional SEM image (left) is because of the vertical growth of the film during deposition, which is typical for RF magnetron sputtering. Such a columnar architecture enhances mechanical stability and crack resistance under cyclic bending because this helps to distribute the stress across the grain boundaries. Good electrical conductivity and optical transparency depend on these granules' continuous and dense network across the surface. The initial resistance of the sheet is about 2.35–2.40 ohms per square. The grain boundaries and dense particle packing suggest the film's mechanical endurance under bending and thermal cycling. The vertical growth and surface homogeneity of the AZO film can be seen in both photos, revealing its structural integrity.

Cycles of bending fatigue cause cracks in AZO thin films placed on flexible substrates, as seen in Figures 4–6. High temperatures increase crack formation. Figure 4 shows the as-produced AZO thin film's surface, before cyclic bending, under an optical microscope. The colors in Figure 4 indicate the changes in reflectivity that were observed under the optical microscope, reflecting the homogeneity of the thin film. Such color changes are due to minor variations in the refractive index across the film. Moreover, the minor dots seen in Figure 5 are related to surface imperfections or particulate matter added during deposition, which had no significant effect on the film's structure. No major cracks or

defects are seen on the surface. Before mechanical stress was applied, this baseline image shows the thin film in its purest state. The AZO thin film after 1200 bending cycles at 23 °C is shown in Figure 5. The arrows in the figure indicate fissures on the film's surface, indicating mechanical fatigue from cyclic bending. The magnified area shows a crack that is still developing but was caused by repeated bending. With riding, these fissures worsen, compromising the thin film's structural integrity. Cracks emerge because of the thin film's tensile and compressive pressures during each cycle. Tensile tension is applied to the outer surface and compression to the inner surface when the film is bent. Cycles of stress and strain degrade the film, causing cracks to form.



Figure 4. Optical microscope image of the as-deposited AZO thin film's surface before any mechanical stress was applied, showing a pristine condition.

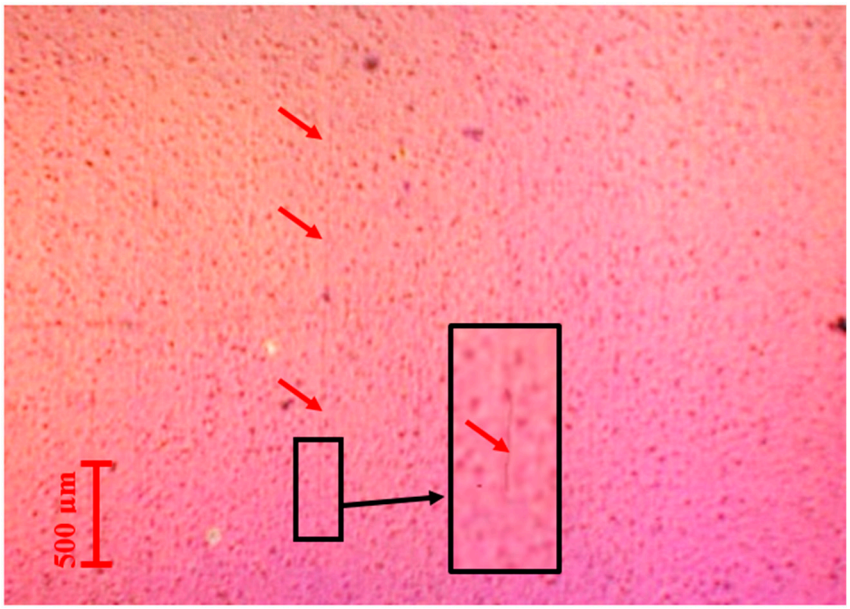


Figure 5. Surface of the AZO film after 1200 bending cycles at 23 °C, showing microcrack formation due to cyclic stress, with enlarged crack area.

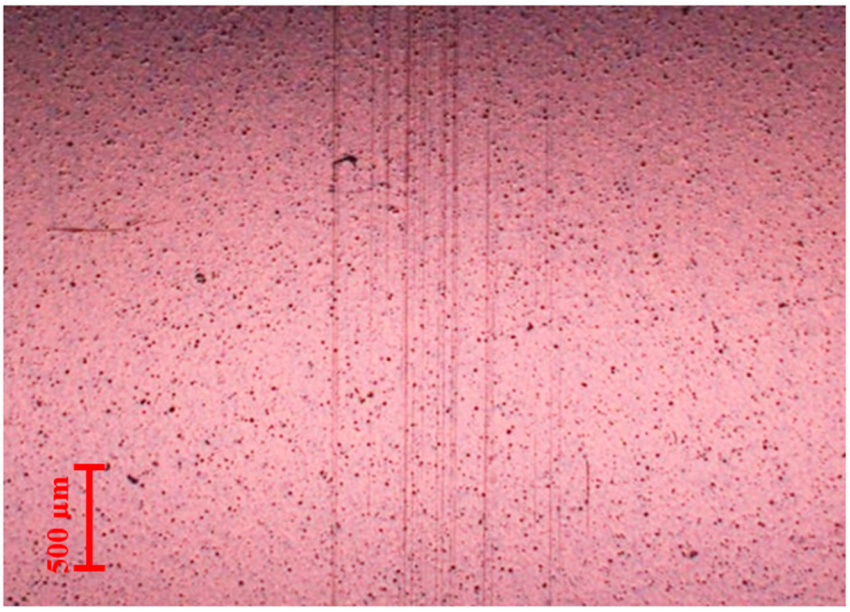


Figure 6. Surface of the AZO film after 1200 bending cycles at 70 °C, showing more extensive cracking compared to that in room temperature samples.

Figure 6 shows the same AZO thin film after 1200 bending cycles at 70 °C. Similar cracks appear more obvious and extensive than those in Figure 7. This suggests that greater temperatures accelerate cracking. Thermal expansion imparts stress to the cyclically loaded thin film at high temperatures. This thermal stress causes microcracks and flaws because higher temperatures lower the material's deformation resistance. The material softens at high temperatures, making it more prone to mechanical deformation and fatigue. Thermal cycling and mechanical stress can accelerate microcrack propagation, especially along grain boundaries, or other thin film vulnerabilities. A scientific explanation for this is that the cyclic mechanical stresses that thin films are subjected to during bending cause cracks. Tensile stress on the convex side and compressive stress on the concave side strain the film's microstructure when bent. Over time, repetitive loading and unloading can cause microscopic flaws to form cracks. Cracks start small but expand as the number of cycles rises, affecting the film's mechanical integrity and, possibly, electrical characteristics.

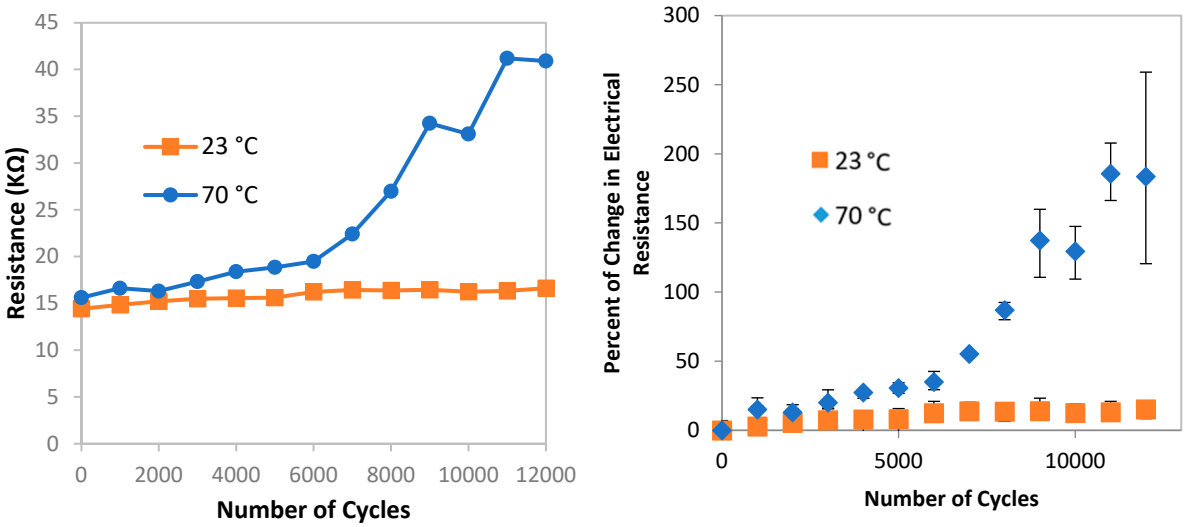


Figure 7. Graphs showing the increases in the electrical resistance (**left**) and the PCER (**right**) with increasing number of cycles for the samples tested at 23 °C and 70 °C.

Materials' thermal and mechanical properties are affected by the temperature, which promotes fracture formation. High temperatures generate thermal expansion, which, when paired with mechanical stress, strains the material. High temperatures increase atomic vibrations, which cause dislocations and microcracks. Thermal softening diminishes mechanical fatigue resistance, accelerating crack propagation under cyclic loads.

Two graphs are presented in Figure 7, with the left graph showing the number of cycles vs. the electrical resistance and the right showing the number of cycles vs. the percentage change in the electrical resistance for samples tested at both 23 °C and 70 °C. Each curve represents the average of five samples. These figures are important for understanding the degradation behavior of AZO thin films subjected to cyclic bending at different temperatures. It can be seen from the left graph that in the case of the samples at 23 °C, the values of the resistance remain rather stable during the cycles. The samples at 70 °C have shown a significant rise in the resistance, especially after 5000 cycles. This trend steepens further beyond 10,000 cycles, hence indicating the rapid electrical breakdown of the AZO coating at high temperatures. The divergence of the resistance curves at 23 °C and 70 °C illustrates how the temperature accelerates degradation; the resistance values are more than 400% higher than those at the ambient temperature. The graph on the right normalizes the changes in the electrical resistance through the use of the PCER, which allows for comparison among the samples because of possible dimensional variations. The PCER is a better measure of reliability because it directly describes the functional degradation of the thin film. By taking it into account, for instance, a 100% gain in the electrical resistance, as would be given by the PCER, would mean that the resistance has doubled, something that is catastrophic as far as performance is concerned for an electronic device. Hence, the PCER is a tool that plays an important role in the long-term and real-life reliability and durability testing of materials.

The PCER data explain the differences in the material's trend variations at the two temperatures. The PCER hardly varies with the increase in the number of cycles, even above 12,000 cycles at 23 °C, indicating that there is very excellent stability in the electrical performance. However, at 70 °C, the PCER increases from 5000 cycles and rapidly increases after more than 10,000 cycles to over 250% after 12,000 cycles. This rapid increase in the PCER at 70 °C indicates severe degradation in the material's electrical properties and would lead to failure in an actual electronic device.

Figures 4–6 show the microscopic crack formation. The trend in Figure 7 is in agreement with the microscopic observations in Figures 4–6. Figure 4 shows the pristine state of the AZO film devoid of any cracks. However, as shown in Figure 5, cracks do form when bending is repeated at room temperature, and this corresponds to the gradual resistance increase seen for the 23 °C samples in the left graph above. This slow crack development limits the resistance increase.

For the 70 °C condition, as shown in Figure 6, such huge increases in the resistance and PCER are directly related to the accelerated creation of cracks, as observed in Figure 6. High temperatures soften the AZO film and increase its susceptibility for crack creation and propagation under cyclic bending. This leads eventually to increased structural damage, clearly noticeable from the big cracks in Figure 6, leading to the sudden increase in the electrical resistance after 10,000 cycles.

The DOE used in this work was a factorial design with the intention to investigate the effects of two factors, namely, the number of cycles and the temperature, on the PCER of AZO thin films undergoing both thermal and mechanical cycling. The NOC had thirteen levels, while the temperature factor had two levels, namely 23 °C and 70 °C. The interaction effect of the NOC and the temperature was also included in the model to see whether the combined effect of both of these factors significantly alters the PCER.

The ANOVA results of the PCER are presented in Table 1. The NOC, temperature, and their interaction (NOC*Temp) were considered as factors in the model. All the *p*-values for the terms in the model (NOC, Temp, and NOC*Temp) are 0.000, thus proving that they are all statistically significant at the 95% confidence level. The F-values are huge, with the

maximum for a temperature factor of 827.89, which indicates that the temperature factor exerts a more remarkable main effect than the other factors on the percentage change in the electrical resistance. Also, the NOC * temperature interaction is significant, with F = 96.06. This means that the effect of the NOC varies with the temperature regarding the PCER and verifies the trends in the previous figure showing significant increases in both the resistance and PCER at 70 °C from 23 °C, specifically when the number of cycles is increased. As indicated in Figure 6, the higher the temperature and the longer the cycling, the greater the increase in the resistance.

Table 1. Analysis of variance for the PCER.

Source	DF	SS	MS	F	*p*
NOC	12	91,808	7650.7	120.55	0.000
Temp	1	52,541	52,541.0	827.89	0.000
NOC*Temp	12	73,157	6096.4	96.06	0.000
Error	52	3300	63.5		
Total	77	220,806			

Table 2 summarizes the model's fit, with R-squared at 98.51% and an adjusted R-squared value of 97.79%. This suggests that much of the variation in the PCER is explained by this model. The low standard deviation, S = 7.96641, further indicates a good model fit, with a low variance in the error. The ANOVA results confirm these trends evident in these figures, especially the interaction between the NOC and the temperature. The resistance curve in Figure 6 therefore indicates that the electrical resistance at an elevated temperature of 70 °C is far greater after a higher number of cycles compared with that at room temperature (23 °C). Furthermore, the PCER at 70 °C exhibits a steep climb, as illustrated on the right-hand side in Figure 6, showing that synergistic loading and thermal exposure caused degradation in the electrical properties of the AZO thin film. We also cannot exclude the possible contribution of the substrate to the observed effects at elevated temperatures. As duly noted by the reviewer, such expansion or softening of the PET substrate might affect the mechanical response of the AZO film as well, in particular, concerning the distribution of stresses upon bending. This could be one plausible factor to take into account when interpreting the performance degradation of the AZO films.

Table 2. Model summary.

S	R-Squared	R-Squared (Adjusted)
7.96641	98.51%	97.79%

The DOE results have clearly pointed out that cycling and the temperature are two critical factors affecting the mechanical stress performance of the AZO thin films, where the temperature is the more important factor. This finding would be important in applications where the AZO films are exposed to ATC because increases in resistance could affect the performance of electronic devices.

Figures 8–10 represent the important roles of the NOC and the temperature in determining the PCER of AZO thin films. These figures reflect the fact that the combined mechanical and thermal stresses accelerate the degradation of the electrical properties of the sputtered films with time.

Figure 8 shows two graphs: left—the number of cycles versus the electrical resistance—and right—the PCER. It is clear from these graphs that at 23 °C, the electrical resistance remains almost constant, even up to 12,000 cycles, while for the samples kept at 70 °C, there is a sharp increase in the resistance after 6000 cycles. This would, in turn, indicate that the higher the temperature, the shorter the degradation process is by that factor. The same is more apparent in the right-hand graph, which plots the PCER as the metric when its value reaches over 250% after 12,000 cycles for the samples tested at 70 °C. Such an

abrupt increase indeed indicates that the accentuation of the damage to the AZO thin films—because cracks are far more major and microstructural changes—may be more apparent, as observed in Figures 4–6, through cyclic bending at elevated temperatures.

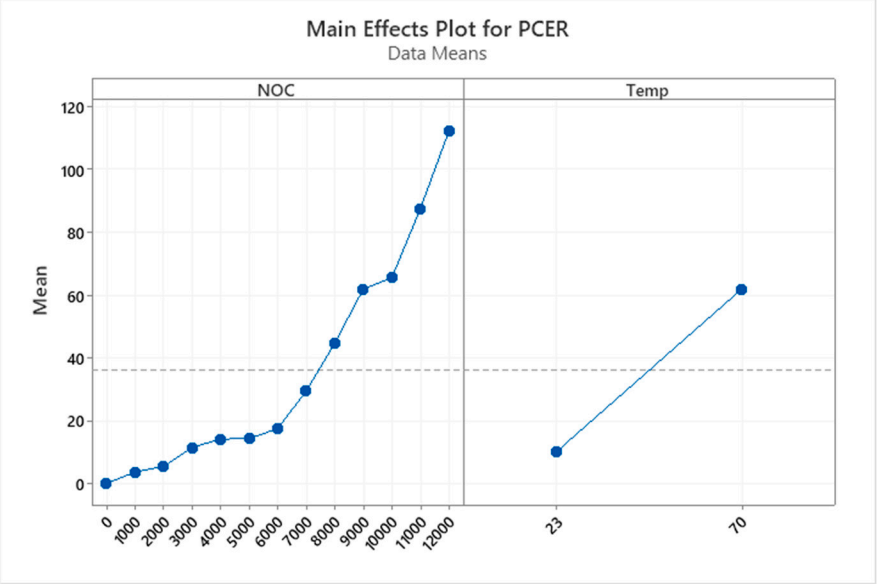


Figure 8. Main effect plots showing the influences of the cycle count and temperature on the PCER.

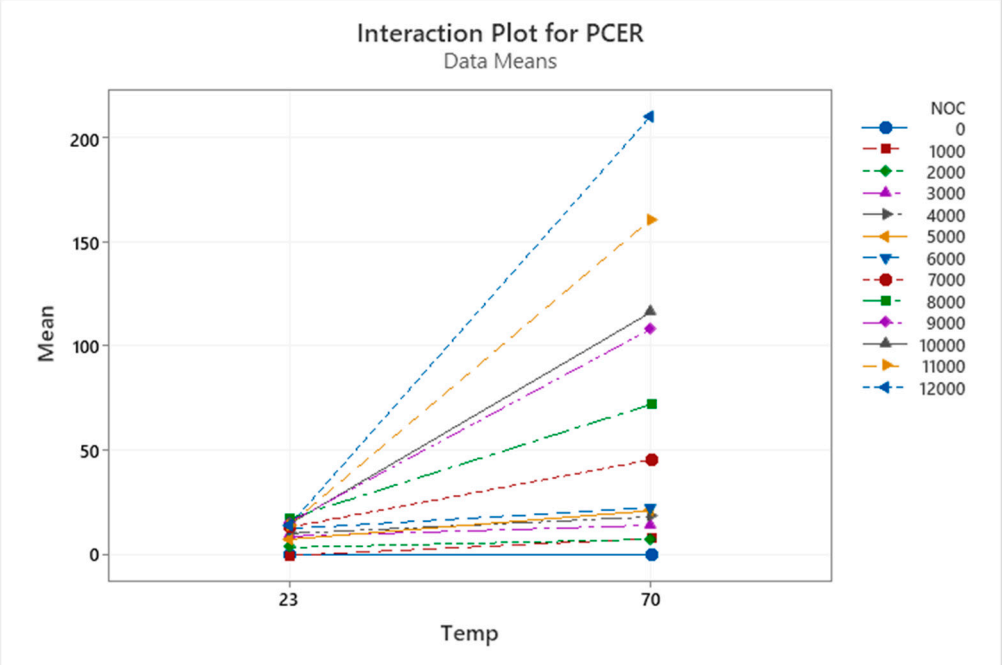


Figure 9. Interaction plot showing the combined effects of the cycle count and the temperature on the PCER.

More insight into the interplay between the NOC and the temperature is provided by Figure 9. Whereas at 23 °C, the increase in the PCER is negligible, even for very prolonged cycling, at 70 °C, the PCER increases substantially, in particular, after 6000 cycles. The interaction plot amplifies the observation that the nonlinear, accelerated degradation of the electrical properties of the films is provoked by high temperatures acting in concert with extensive cycling. From this, it could be surmised that thermal stress augments the effects of mechanical fatigue by probably softening the material of the AZO film and making

it more susceptible to crack propagation and microstructural defects. This, indeed, is a statistically significant interaction, as seen in the ANOVA results in Table 1 for the strongly significant effects of the main factor of the NOC and the temperature and their interaction.

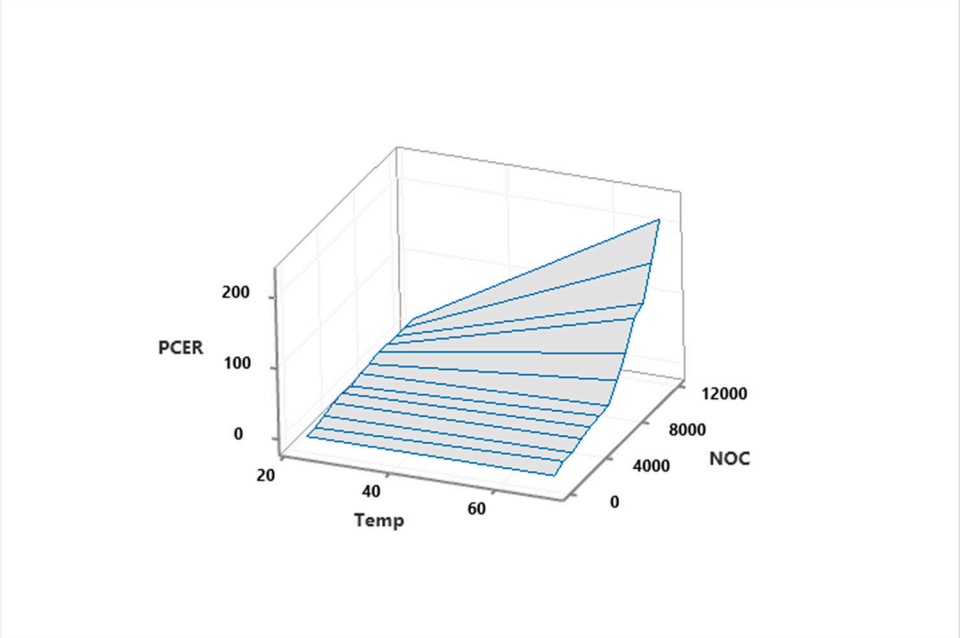


Figure 10. Three-dimensional surface plot showing the relationship among the cycle count, temperature, and PCER.

Figure 10 shows the 3D surface plot showing the combined effects of the NOC and the temperature on the PCER. As seen, the surface slopes steeply upward for increasing temperature and NOC, reflecting rapid degradation under elevated conditions of both factors. This plot makes it clear that consideration of both mechanical and thermal stresses is important for the evaluation of the durability of AZO thin films for application in flexible electronics. Low cycle counts or room temperature conditions result in minor degradations, but the combination of high temperatures and high cycle counts produces a marked increase in the PCER, confirming further that this material is indeed vulnerable under combined stresses. The surface plot emphasizes nonlinear degradation behavior because modest increases in either the NOC or the temperature do not have as drastic an effect as their combination.

In other words, the detailed tendencies displayed in Figs. 8–10 show that AZO thin films can withstand moderate mechanical and thermal stresses separately, but under the joint action of high temperatures and extended cyclic bending, their electrical properties undergo severe degradation. The obtained results are very important for the application of AZO films in flexible electronics, where such conditions of the environment are often encountered. The data show that there is a high potential for enhancing longevity and reliability in these devices by mitigating temperature effects on AZO films.

Figure 11 shows the PCER of the AZO thin films with respect to the NOC after the ATC experiment. After 500 heating cycles, the PCER is higher than 300%, demonstrating a certain tendency of incrementation in the electrical resistance. This high increase in the electrical resistance is in good agreement with the repetitive heat stress degrading the electrical characteristics of the AZO thin film. In the first part of the test with fewer cycles, the PCER increases very little. This shows that the resistance increases rapidly after 100 cycles, with very large surges between 300 and 500 cycles. Considering the thermal cycling due to microstructural changes in the thin films, the error bars indicate some fluctuations.

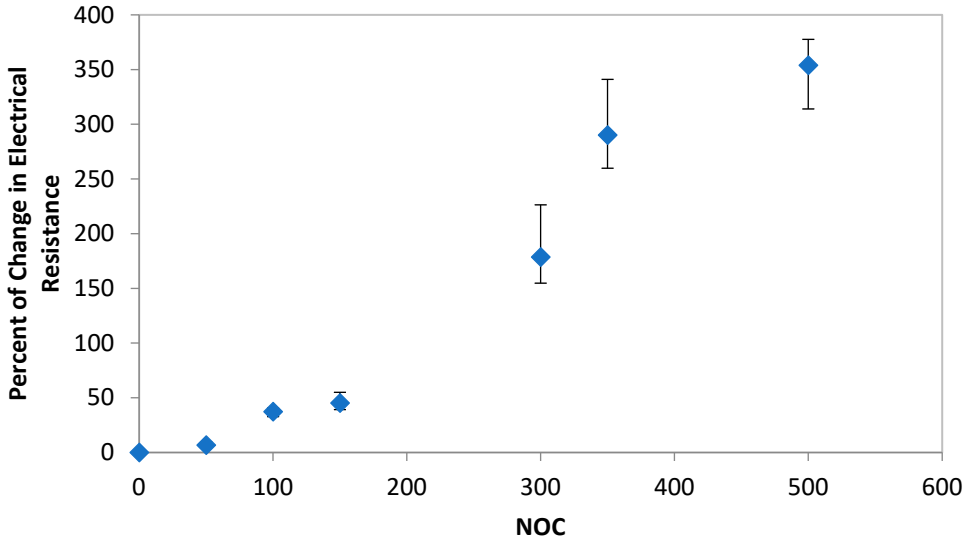


Figure 11. PCER of AZO thin films as a function of the number of thermal cycles, showing a sharp increase after 300 cycles.

The AZO film expands and compresses during thermal cycling, increasing the electrical resistance. Each heating cycle followed by cooling creates thermal stress that could result in microcracking, voids, and grain boundary instabilities in the thin film. Such microstructural changes provide additional pathways for increasing the resistivity of the film, thus decreasing the electrical conductivity and increasing the electrical resistance. In such temperature cycling, partial delamination may occur between the film and its substrate, which increases the resistance. This high spike in the PCER after 300 cycles may be a threshold beyond which microcracks and flaws have accumulated enough to cause very rapid degradation of the electrical performance. It is seen that thin film materials under thermal cycling undergo an initial period of gradual degradation followed by an accelerated phase, where the materials' structure is progressively degraded. Heat cycling and cyclic bending fatigue experiments show similar degradation trends, though driven by different stress mechanisms. As indicated in the previous figures, during the bending fatigue experiment, the electrical resistance increased as a function of the number of mechanical flexing cycles—particularly at high temperatures. In other words, the defects and deformation of the AZO layer, because of mechanical strain under cyclic bending, lead to a decrease in the electrical conductivity.

Thermal cycling and bending fatigue both cause flaws, microcracks, and grain boundary disruptions that hamper electron transport and increase resistance. Above a threshold (300 heat cycles in Figure 11 and 6000 bending cycles in Figure 8), degradation accelerates, demonstrating the importance of thermal and mechanical stressors for AZO thin films' integrity. Both investigations show that environmental and mechanical aspects must be considered when applying AZO thin films, especially in flexible electronics or heat cycling and mechanical strain situations. Thermal cycling research suggests that thermal and mechanical fatigue degradation processes are similar, making it important to account for both effects in film design and use in real-world devices.

4. Conclusions

The present study deals with detailed mechanical and thermal endurance tests of AZO thin films, deposited on PET substrates, under combined cyclic bending fatigue and thermal cycling conditions. These results clearly suggest that high temperatures and longer mechanical stresses significantly affect the electrical and structural properties of AZO films. At room temperature (23 °C), the films were quite stable, showing less than a 50% increase in the PCER after 12,000 cycles. However, the PCER at 70 °C was already hugely increased and more than 250% under the same conditions, indicating accelerated degradation due to

thermal effects. Moreover, thermal cycling between 0 and 100 °C resulted in more than a 300% increase in the PCER after 500 cycles, which is evidence that thermal expansion and contraction can cause microstructural variations, inducing performance degradation.

Indeed, this analysis confirmed that both the number of bending cycles and the temperature were significant factors, and the effect of the interaction between these factors on the electrical resistance of the films was strong. These results underline the importance of considering combined mechanical and thermal stressors in the design of AZO films for flexible electronics. In addition, this study shows that optimization techniques in deposition and the addition of protective coatings might be further developments for obtaining AZO films that are more reliable in real-life applications. Future research on alternative doping methods, advanced processes for deposition, and multilayer architectures may improve AZO films' stability and performance under hostile environmental conditions.

Author Contributions: Conceptualization, M.M.H.; methodology, M.M.H. and K.A.; writing—original draft preparation, all the authors. All authors have read and agreed to the published version of the manuscript.

Funding: The research publication fees (APC) are funded by Auburn University, USA.

Data Availability Statement: The data are available on request.

Acknowledgments: The authors would like to acknowledge Auburn University for their support to publish this work.

Conflicts of Interest: The authors declare that they have no conflicts of interest in relation to the work described in this manuscript. This includes, but is not limited to, financial interests, personal relationships, or affiliations that could be perceived to influence or bias this work.

References

1. Hamelmann, F.U. Transparent conductive oxides in thin film photovoltaics. *J. Phys. Conf. Ser.* **2014**, *559*, 012016. [CrossRef]
2. Fortunato, E.; Ginley, D.; Hosono, H.; Paine, D.C. Transparent conducting oxides for photovoltaics. *MRS Bull.* **2007**, *32*, 242–247. [CrossRef]
3. Beyer, W.; Hüpkes, J.; Stiebig, H. Transparent conducting oxide films for thin film silicon photovoltaics. *Thin Solid Films* **2007**, *516*, 147–154. [CrossRef]
4. Chae, G.S. A modified transparent conducting oxide for flat panel displays only. *Jpn. J. Appl. Phys.* **2001**, *40*, 1282. [CrossRef]
5. Oh, B.-Y.; Jeong, M.-C.; Moon, T.-H.; Lee, W.; Myoung, J.-M.; Hwang, J.-Y.; Seo, D.-S. Transparent conductive Al-doped ZnO films for liquid crystal displays. *J. Appl. Phys.* **2006**, *99*, 122110. [CrossRef]
6. Yan, M.; Zhang, Q.; Zhao, Y.; Yang, J.; Yang, T.; Zhang, J.; Li, X. Applications of transparent conducting oxides in organic light-emitting devices. *J. Nanosci. Nanotechnol.* **2015**, *15*, 6279–6294. [CrossRef]
7. Jaakkola, K.; Tappura, K. Exploitation of transparent conductive oxides in the implementation of a window-integrated wireless sensor node. *IEEE Sens. J.* **2018**, *18*, 7193–7202. [CrossRef]
8. Afre, R.A.; Sharma, N.; Sharon, M.; Sharon, M. Transparent conducting oxide films for various applications: A review. *Rev. Adv. Mater. Sci.* **2018**, *53*, 79–89. [CrossRef]
9. Ganose, A.M.; Scanlon, D.O. Band gap and work function tailoring of SnO_2 for improved transparent conducting ability in photovoltaics. *J. Mater. Chem. C* **2016**, *4*, 1467–1475. [CrossRef]
10. Shankar, U.; Oberoi, D.; Bandyopadhyay, A. A review on the alternative of indium tin oxide coated glass substrate in flexible and bendable organic optoelectronic devices. *Polym. Adv. Technol.* **2022**, *33*, 3078–3111. [CrossRef]
11. Almuslem, A.S.; Shaikh, S.F.; Hussain, M.M. Flexible and stretchable electronics for harsh-environmental applications. *Adv. Mater. Technol.* **2019**, *4*, 1900145. [CrossRef]
12. Alkhazaili, A.; Hamasha, M.M.; Choi, G.; Lu, S.; Westgate, C.R. Reliability of thin films: Experimental study on mechanical and thermal behavior of indium tin oxide and poly(3,4-ethylenedioxythiophene). *Microelectron. Reliab.* **2015**, *55*, 538–546. [CrossRef]
13. Wang, G.; Gao, E.; Dai, Z.; Liu, L.; Xu, Z.; Zhang, Z. Degradation and recovery of graphene/polymer interfaces under cyclic mechanical loading. *Compos. Sci. Technol.* **2017**, *149*, 220–227. [CrossRef]
14. Cao, Q.; Rogers, J.A. Ultrathin films of single-walled carbon nanotubes for electronics and sensors: A review of fundamental and applied aspects. *Adv. Mater.* **2009**, *21*, 29–53. [CrossRef]
15. Finn, M., III; Martens, C.J.; Zaretski, A.V.; Roth, B.; Søndergaard, R.R.; Krebs, F.C.; Lipomi, D.J. Mechanical stability of roll-to-roll printed solar cells under cyclic bending and torsion. *Sol. Energy Mater. Sol. Cells* **2018**, *174*, 7–15. [CrossRef]
16. Kim, T.-W.; Lee, J.-S.; Kim, Y.-C.; Joo, Y.-C.; Kim, B.-J. Bending strain and bending fatigue lifetime of flexible metal electrodes on polymer substrates. *Materials* **2019**, *12*, 2490. [CrossRef]

17. Gunda, M.; Kumar, P.; Katiyar, M. Review of mechanical characterization techniques for thin films used in flexible electronics. *Crit. Rev. Solid State Mater. Sci.* **2017**, *42*, 129–152. [CrossRef]
18. Peng, C.Y.; Ye, L.; Lu, S.; Westgate, C.R. Electrical and optical degradation studies on AZO thin films under cyclic bending conditions. *IEEE Trans. Device Mater. Reliab.* **2013**, *13*, 236–244. [CrossRef]
19. Hamasha, M.M.; Lu, S.; Westgate, C.R. Stability of ITO thin film on flexible substrate under thermal aging and thermal cycling conditions. *J. Disp. Technol.* **2012**, *8*, 385–390. [CrossRef]
20. Dhakal, T.P.; Lu, S.; Vasekar, P.; Westgate, C.R. Moisture-induced surface corrosion in AZO thin films formed by atomic layer deposition. *IEEE Trans. Device Mater. Reliab.* **2012**, *12*, 347–356. [CrossRef]
21. Nozaki, Y.; Lerche, D.; Alibo, D.S.; Tsutsumi, M. Dissolved indium and rare earth elements in three Japanese rivers and Tokyo Bay: Evidence for anthropogenic Gd and In. *Geochim. Cosmochim. Acta* **2000**, *64*, 3975–3982. [CrossRef]
22. Wen, L.; Sahu, B.B.; Kim, H.R.; Han, J.G. Study on the electrical, optical, structural, and morphological properties of highly transparent and conductive AZO thin films prepared near room temperature. *Appl. Surf. Sci.* **2019**, *473*, 649–656. [CrossRef]
23. Zhang, Y.; Yang, Y.; Zhao, J.; Tan, R.; Wang, W.; Cui, P.; Song, W. Optical and electrical properties of aluminum-doped zinc oxide nanoparticles. *J. Mater. Sci.* **2011**, *46*, 774–780. [CrossRef]
24. Zhou, H.; Yi, D.; Yu, Z.; Xiao, L.; Li, J. Preparation of aluminum doped zinc oxide films and the study of their microstructure, electrical and optical properties. *Thin Solid Films* **2007**, *515*, 6909–6914. [CrossRef]
25. Tahar, R.B.H. Structural and electrical properties of aluminum-doped zinc oxide films prepared by sol–gel process. *J. Eur. Ceram. Soc.* **2005**, *25*, 3301–3306. [CrossRef]
26. Jeong, S.H.; Boo, J.H. Influence of target-to-substrate distance on the properties of AZO films grown by RF magnetron sputtering. *Thin Solid Films* **2004**, *447*, 105–110. [CrossRef]
27. Fang, G.; Li, D.; Yao, B.L. Fabrication and vacuum annealing of transparent conductive AZO thin films prepared by DC magnetron sputtering. *Vacuum* **2002**, *68*, 363–372. [CrossRef]
28. Bosco, J.; Tajdar, F.; Atwater, H. Molecular beam epitaxy of n-type ZnS: A wide band gap emitter for heterojunction PV devices. In Proceedings of the 2012 38th IEEE Photovoltaic Specialists Conference, Austin, TX, USA, 3–8 June 2012; pp. 2513–2517.
29. Alyamani, A.; Tataroğlu, A.D.E.M.; El Mir, L.; Al-Ghamdi, A.A.; Dahman, H.; Farooq, W.A.; Yakuphanoğlu, F. Photoresponse and photocapacitor properties of Au/AZO/p-Si/Al diode with AZO film prepared by pulsed laser deposition (PLD) method. *Appl. Phys. A* **2016**, *122*, 297. [CrossRef]
30. Znaidi, L.; Touam, T.; Vrel, D.; Souded, N.; Yahia, S.B.; Brinza, O.; Fischer, A.; Boudrioua, A. AZO thin films by sol-gel process for integrated optics. *Coatings* **2013**, *3*, 126–139. [CrossRef]
31. Liang, G.-X.; Fan, P.; Cai, X.-M.; Zhang, D.-P.; Zheng, Z.-H. The influence of film thickness on the transparency and conductivity of Al-doped ZnO thin films fabricated by ion-beam sputtering. *J. Electron. Mater.* **2011**, *40*, 267–273. [CrossRef]
32. Hamasha, M.M.; Dhakal, T.P.; Vasekar, P.; Alzoubi, K.; Lu, S.; Vanhart, D.; Westgate, C.R. Reliability of sputter deposited aluminum-doped zinc oxide under harsh environmental conditions. *Sol. Energy* **2013**, *89*, 54–61. [CrossRef]

Disclaimer/Publisher's Note: The statements, opinions and data contained in all publications are solely those of the individual author(s) and contributor(s) and not of MDPI and/or the editor(s). MDPI and/or the editor(s) disclaim responsibility for any injury to people or property resulting from any ideas, methods, instructions or products referred to in the content.